Analysis and Design of a Historical Bicycle Mechanism, Without Chain

Sebastian Coltescu(✉) and Simona-Mariana Cretu

Faculty of Mechanics, University of Craiova, Calea Bucuresti 107, Craiova, Romania
sebi_c82@yahoo.com

Abstract. The aim of this study is to make the kinematic analysis and to design a historical mechanism for the bicycle, without chain, only with links. The relationships between the angular stroke of the pedal rockers and the geometric parameters of the mechanism are established in order to achieve the synthesis and optimization of the mechanism. The geometric model was made with the Autodesk Inventor program and the kinematic analysis with the Altair Inspire program. The engine was placed in the crank-base joint, considering the intention to use the mechanism for medical purposes in the future.

Keywords: bicycle link mechanism · kinematic analysis · critical positions · Altair Inspire

1 Introduction

People have always been interested in developing mechanisms to facilitate day-to-day activities, such as fast moving. The history of the bicycle is interesting and can be said to extend from 1418 to the present day. A brief history of the bicycle is presented in [1].

Giovanni Fontana built in 1418 the first four-wheeled human-powered vehicle. In 1790, the French count Sivrac invented the Celerifery with two wooden wheels, and the movement was done by pushing with feet on the ground. The Velocipede is supposed to have been invented in 1818 by the German Baron Karl von Drais, and moved according to the same principle as Celerifery [2, 3].

Scottish blacksmith Kirkpatrick MacMillan invented a wooden bicycle in 1839 ([4], Fig. 1a) and Thomas McCall built a replica of it in 1896; the last there is in the Dumfries Museum ([3], Fig. 1b). The MacMillan's bicycle had a link mechanism, operated by man through the pedals, thus avoiding touching the ground. The drive elements, on which the pedals are placed, perform an oscillating movement; the movement is transmitted by means of the connecting rods to a crank fixed on the rear wheel.

Over time, other bicycle link mechanisms have been invented (e.g. Chebyshev's bicycle [5, 6]), and their use has been extended to the present day.

The evolution of the bicycle until the current period surprises through technological, mechanical and actuation novelties; there are for example electric bicycles, very light, having the possibility to reach speeds of over 50 km/h, or bicycles with the shifter built into the hub.

© The Author(s) 2023
I. Dumitru et al. (Eds.): ICOME 2022, AHE 15, pp. 138–148, 2023.
https://doi.org/10.2991/978-94-6463-152-4_16

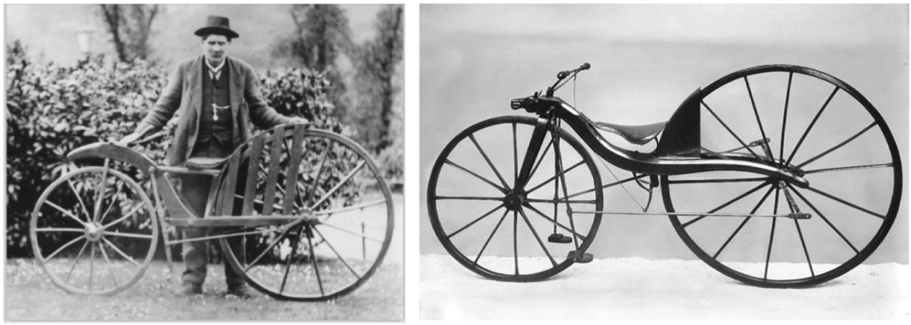

a b

Fig. 1. a) MacMillan's bicycle with link mechanism [4]; b) Thomas McCall's bicycle (MacMillan's bicycle replica) [3].

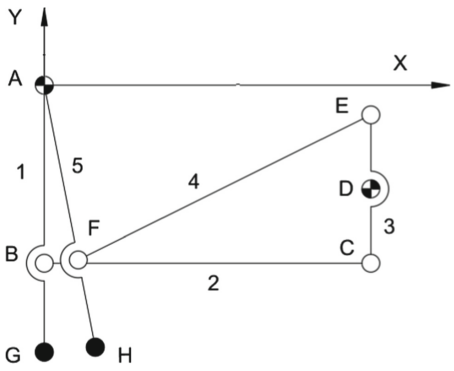

Fig. 2. Kinematic scheme of the bicycle mechanism.

In 1903, two companies, Sturmey Archer and Sachs, launched some hubs with built-in derailleur. They have many advantages, of which we can remind avoid the fall of the chain and the automatic change of gears. Currently, bicycles with link mechanisms with/without built-in hubs are manufactured [7].

Given the interest in link mechanisms used at bicycles, the field of study remains relevant [8–10].

This paper deals with the analysis and design of the historical mechanism of Kirkpatrick MacMillan.

2 Analysis of the Bicycle Link Mechanism

2.1 Structural Analysis

The kinematic scheme of the mechanism is shown in Fig. 2.

The geometric data for this mechanism, as a replica of the MacMillan's bicycle, are the following:

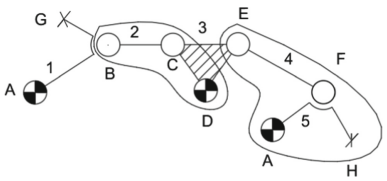

Fig. 3. Structural scheme of the bicycle mechanism.

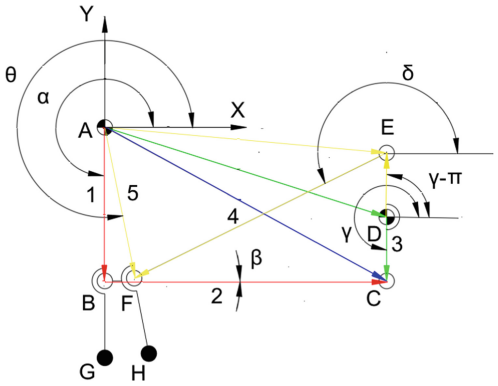

Fig. 4. Vector diagram for kinematic analysis.

$l_{AB} = 240$ mm, $l_{AG} = 360$ mm, $l_{BC} = 440$ mm, $l_{EC} = 200$ mm, $l_{EF} = 440$ mm, $l_{AF} = 240$ mm, $l_{AH} = 360$ mm, $x_A = 0$ mm, $y_A = 0$ mm; $x_D = 440$ mm, $y_D = -140$ mm.

The mechanism is decomposed according to Assur's principle into the driving element 1 and two RRR dyads (BCD and EFA, Fig. 3).

2.2 Kinematical Analysis

For the calculation of linear and angular positions, the vector sum equations (Fig. 4) and their projections on the Ox and Oy axes are used (Eq. 1–Eq. 9). All the schemes are made with AutoCAD program [11], for the comparison of the results obtained by the analytical calculation.

$$\begin{cases} x_B = l_{AB} \cdot \cos(\alpha) \\ y_B = l_{AB} \cdot sin(\alpha) \end{cases} \tag{1}$$

$$\begin{cases} x_G = l_{AG} \cdot \cos(\alpha) \\ y_G = l_{AG} \cdot sin(\alpha) \end{cases} \tag{2}$$

$$\overline{AC} = \overline{AB} + \overline{BC} = \overline{AD} + \overline{DC} \tag{3}$$

$$\begin{cases} x_C = x_B + l_{BC} \cdot \cos(\beta) = x_D + l_{DC} \cdot cos(\gamma) \\ y_C = y_B + l_{BC} \cdot sin(\beta) = y_D + l_{DC} \cdot sin(\gamma) \end{cases} \tag{4}$$

$$\overline{AE} = \overline{AD} + \overline{DE} \tag{5}$$

$$x_E = x_D + l_{DE} \cdot \cos(\gamma - 180) \tag{6}$$

$$y_E = y_D + l_{DE} \cdot \sin(\gamma - 180) \tag{7}$$

$$\overline{AF} = \overline{AE} + \overline{EF} \tag{8}$$

$$\begin{cases} x_F = x_E + l_{EF} \cdot \cos(\delta) = l_{AF} \cdot \cos(\theta) \\ y_F = y_E + l_{EF} \cdot \sin(\delta) = l_{AF} \cdot \sin(\theta) \end{cases} \tag{9}$$

Using the Maple 2021 program [12], the kinematic analysis of the mechanism is performed, based on the previously written equations. After running this program, having as input data the geometric dimensions of the mechanism, the following data were obtained:

xb = 0; yb = 240 mm; xc = 440 mm; yc = -240 mm; xe = 440 mm; ye = -40 mm; xf = 45.86564508 mm; yf = -235.57996 mm; β = 0 rad; γ = -1.570796 rad; δ = -1.37854 rad; θ = -2.680980 rad.

2.3 Establishing Limit Positions of the Rocker

When determining the left/right limit positions of the rocker and the coresponding ones of the crank, the critical positions of the mechanism are taken into account when the connecting rod and the crank are collinear, in extension, or overlapping, respectively. The constructions are made using the AutoCAD program (Fig. 5, Fig. 6 and Fig. 7).

The left/right limit positions of the rocker element were analitical calculated with Maple 2021 program.

The coordinates of point B_1 are determined by solving a system of two equations, the equation of the circle with the center at point A of radius AB, and the equation of the circle with the center in D with the radius BC-CD (Eq. 10).

To determinate the coordinates of point B_2, also a system of two equations is solved, the equation of the circle with the center at point A of radius AB, and the equation of the circle with the center in D with the radius $BC + CD$ (Eq. 11).

$$solve(\left\{x^2 + y^2 = lab^2, (x - xd)^2 + (y - yd)^2 = (lbc - lcd)^2\right\}, \{x, y\}); \tag{10}$$

$$solve(\left\{x^2 + y^2 = lab^2, (x - xd)^2 + (y - yd)^2 = (lbc + lcd)^2\right\}, \{x, y\}); \tag{11}$$

The rocker angles for the left/right limit positions were also determined using Ec. 12, i.e. 23,0351863° and 26,79742757° respectively.

$$\widehat{B_iAB} = arctg\left(\frac{x_B}{y_B}\right) \quad i = 1, 2 \tag{12}$$

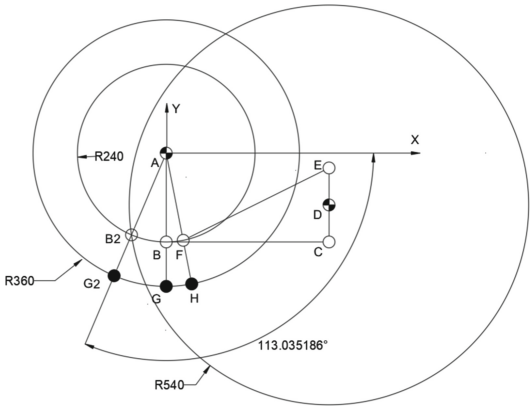

Fig. 5. The scheme for left limit position of the rocker.

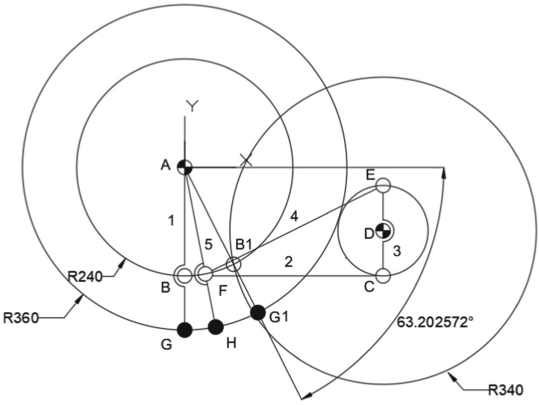

Fig. 6. The scheme for right limit position of the rocker.

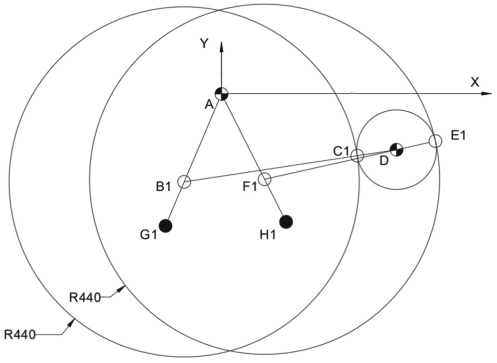

Fig. 7. The positions of the crank corresponding to the limits of the rocker.

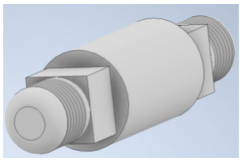

Fig. 8. The crank connection shaft.

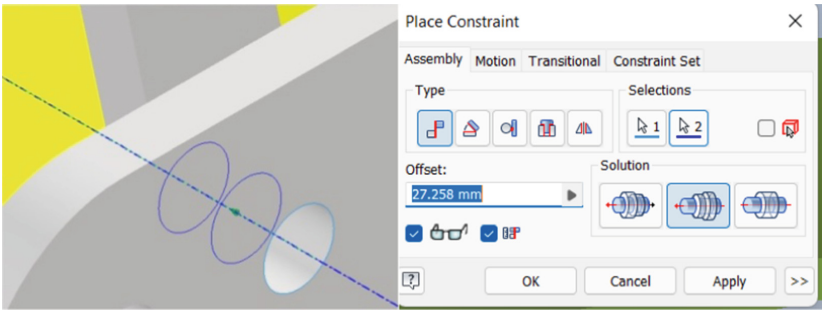

Fig. 9. The constraint of cylindrical surfaces.

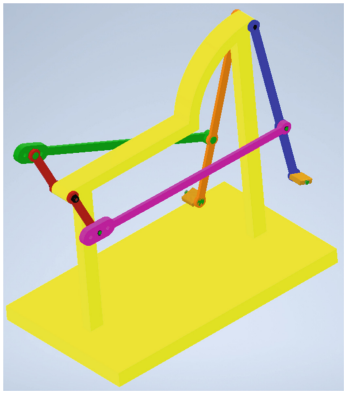

Fig. 10. The final model made in the Inventor program.

2.4 Kinematic Analysis with Altair Inspire Program

The mechanism was modeled with the Inventor program [13]. The shaft used for the rigid assembly of the two cranks in the Fig. 8 is shown.

The constraints between the *Parts* were defined by alignment on the axes and on the surfaces, in order to create the kinematic hinges; in Fig. 9 it can be seen the constraint of cylindrical surfaces.

The final geometrical model of the mechanism, made in the Inventor program in Fig. 10 is presented.

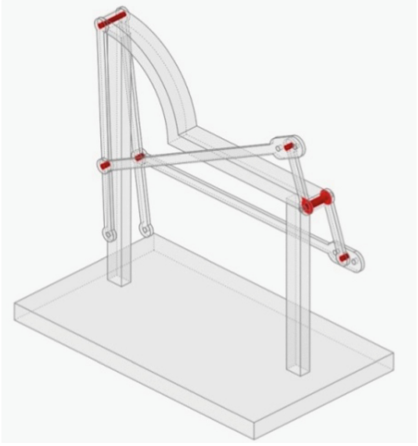

Fig. 11. The joints from the mechanism.

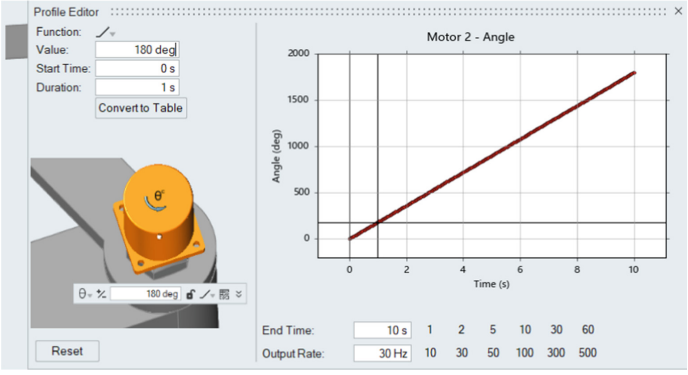

Fig. 12. Engine positioning in the crank-base hinge and the parameters of the motor.

The file exported from the Inventor program it was imported into the Altair Inspire program [14], for kinematic analysis.

The direction of gravity is indicated.

The crank elements and the connecting shaft were assembled as rigid elements by means of *Rigid Element* command and the base becomes fixed with the command *Ground*.

All kinematic joints in the mechanism have been selected as hinges, with the *Joints* command (Fig. 11).

The engine positioned in the joint between the crank and the base has a constant speed of 180 degrees per second, so that the rocker of the mechanism performs 2 strokes (front/rear) in two seconds. For this, double-click the engine and select the *Ramp* type, with the following parameters of the function: *Value 180* deg*, Start time 0*, *Duration 1* s*;* select the time for movement analysis *End time 10* s, and *Output Rate* 30 Hz (Fig. 12).

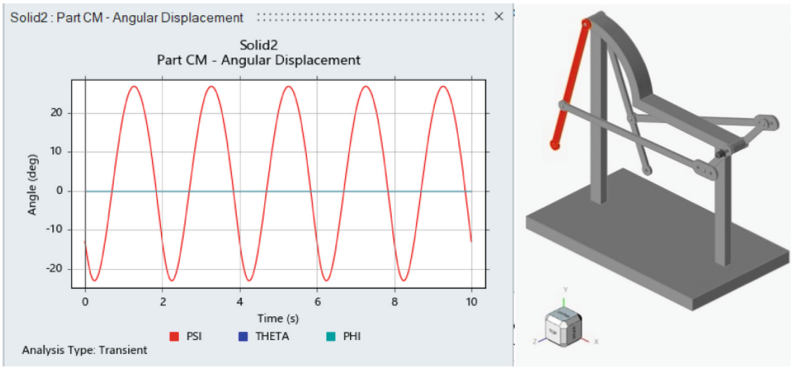

Fig. 13. Angular displacement of the rocker.

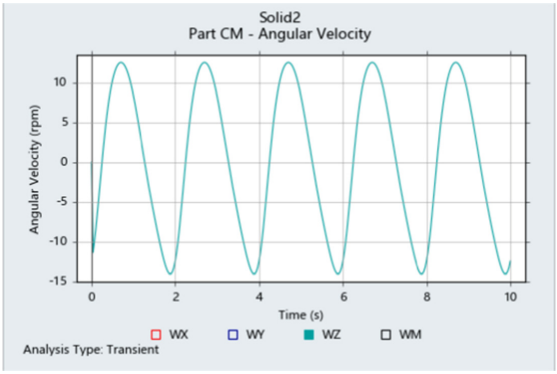

Fig. 14. Angular velocity of the rocker.

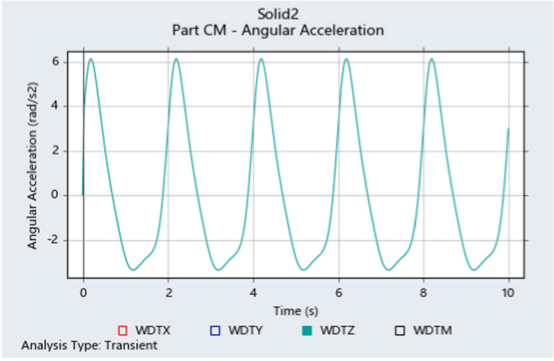

Fig. 15. Angular acceleration of the rocker.

Through the *Motion Analysis* command, the animation of the mechanism is accomplished. Angular displacements, angular velocities and angular accelerations of the rocker element are shown in Fig. 13, 14 and 15 respectively.

The angular positions and the times for forward and backward movement of the rocker arm were verified in the displacement diagrams (Fig. 16). The total time for this

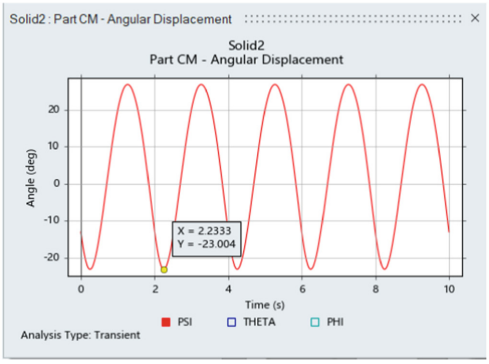

a

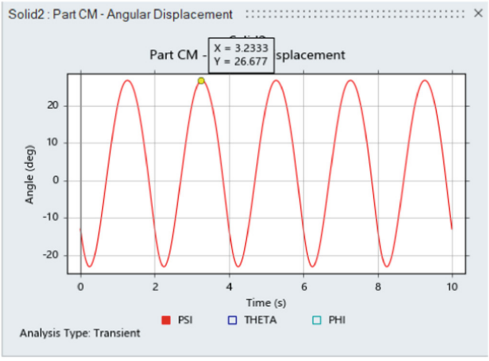

b

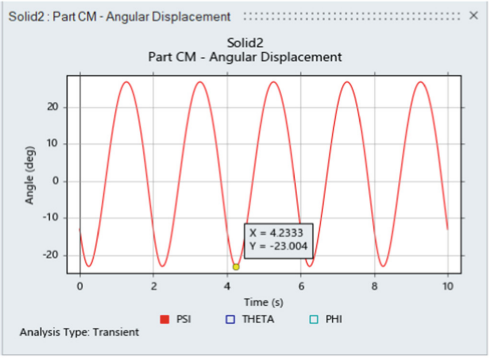

c

Fig. 16. Time and angles for the front/rear stroke.

stroke was obtained as one second (3.2333 s–2.2333 s), and the angle from the vertical axis to the front/rear limit position was 23.004° and 26,677° respectively.

The total time for backward-forward stroke was obtained as one second (4.2333 s–3.2333 s).

3 Conclusions

Given the current interest in bicycles without chain, also used in the medical field, the study aims to start research with historical mechanisms, for the analysis and optimization of this type of mechanical systems. The kinematic analysis of the historical link mechanism for bicycle, invented by Kirkpatrick MacMillan, was performed, both by classical methods and with high-performance programs, and the validity of the model's operation was confirmed. The critical operating positions of the mechanism, when some elements are collinear, have been established, and it has been concluded that it is preferable to place the actuating element in the rotating joint of the crank for medical purposes, which implies the continuation of the study as a problem of synthesis of the function generating mechanism. In order to actuate the rocking element, being necessary to exceed the critical positions, two motors and optimization are required.

References

1. Malppan, G.J, Sunny, T.: A Review on Design Developments in Bicycle. International Research Journal of Engineering and Technology (IRJET) 02 (3), 1794-1799 (2015).
2. https://www.timetoast.com/timelines/evolution-of-the-bicycle-6147ba69-fd0a-4b5d-bf62-6424d176a825, last accessed 2022/04/9.
3. http://www.clg-fort-montlhery.ac-versailles.fr/IMG/pdf/petite_histoire_du_velo.pdf, last accessed 2022/04/9.
4. https://alchetron.com/Kirkpatrick-Macmillan; last accessed 2022/04/9.
5. Artobolevsky, I.I., Levitsky, N. I.: Mechanisms of P. L. Chebyshev. In the book: Scientific heritage of P. L. Chebyshev. Issue. II. Theory of mechanisms. - M.-L.: Academy of Sciences, USSR, pp. 34–35 (1945).
6. Artobolevsky, I.I., Levitsky, N. I.: Models of mechanisms of P. L. Chebyshev. In: Complete works of P. L. Chebyshev. Volume IV. Theory of mechanisms. - M.-L.: Academy of Sciences, USSR, pp. 219–220 (1948).
7. http://mapage.noos.fr/ptis.trucs.sympas/vitesses_dans_le_moyeu.htm, last accessed 2022/04/9.
8. https://www.youtube.com/watch?v=1gFtIyjnFAA, last accessed 2022/04/9.
9. https://www.youtube.com/watch?v=2XM4utsZ49s, last accessed 2022/04/9.
10. https://www.youtube.com/watch?v=7prq2wV24tk, last accessed 2022/04/9.
11. https://knowledge.autodesk.com/support/autocad, last accessed 2022/04/9.
12. https://www.maplesoft.com/support/help/Maple, last accessed 2022/04/9.
13. https://help.autodesk.com/view/INVNTOR/2021/ENU/, last accessed 2022/04/9.
14. https://2021.help.altair.com/2021.2/inspire/en_us/index.htm, last accessed 2022/04/9.

Open Access This chapter is licensed under the terms of the Creative Commons Attribution-NonCommercial 4.0 International License (http://creativecommons.org/licenses/by-nc/4.0/), which permits any noncommercial use, sharing, adaptation, distribution and reproduction in any medium or format, as long as you give appropriate credit to the original author(s) and the source, provide a link to the Creative Commons license and indicate if changes were made.

The images or other third party material in this chapter are included in the chapter's Creative Commons license, unless indicated otherwise in a credit line to the material. If material is not included in the chapter's Creative Commons license and your intended use is not permitted by statutory regulation or exceeds the permitted use, you will need to obtain permission directly from the copyright holder.